J Low Temp Phys (2008) 153: 244–249
DOI 10.1007/s10909-008-9828-0

Stacking Fault Energy in ^{4}He Crystals

H.J. Junes · H. Alles · M.S. Manninen · A.Y. Parshin · I.A. Todoshchenko

Received: 31 May 2008 / Accepted: 27 August 2008 / Published online: 9 October 2008

Abstract Recently observed non-classical rotational inertial (NCRI) in solid ^{4}He is most probably related to defects which appear during the sample preparation. We have measured the energy of the stacking fault (SF) in an hcp ^{4}He crystal at 0.2 K. The SF creates a groove with a dihedral angle of $155 \pm 5°$ on the crystal surface in a quasi-equilibrium with the liquid. The obtained value for the SF energy is (0.07 ± 0.02) mJ/m^2, which is ∼0.4 of the surface tension of the liquid–solid interface of ^{4}He. Our findings suggest that the phenomenon of burst-like creation of new atomic layers might be accompanied by the creation of SFs.

Keywords Helium-4 · Quantum crystals · Liquid–solid interfaces · Stacking faults · Planar defects · Growth kinetics

PACS 61.72.Nn · 67.80.bf

1 Introduction

Disorder in solid ^{4}He has been shown to play an essential role in "supersolidity" [1], the phenomenon first observed by Kim and Chan in 2004 [2, 3] what could be a mass flow through solid ^{4}He. In understanding quantum defects, it is of particular importance to study single well-defined defects [4]. Stacking fault (SF) is a low-energy planar defect in a crystal, which may appear in a ^{4}He crystal in the course of the crystal growth. In contrast to grain boundaries (GBs), the orientation of a SF

H.J. Junes (✉) · H. Alles · M.S. Manninen · I.A. Todoshchenko
Low Temperature Laboratory, TKK, Puumiehenkuja 2B, 02015 Espoo, Finland
e-mail: heikki.junes@ltl.tkk.fi

A.Y. Parshin
P.L. Kapitza Institute, Kosygina 2, Moscow 119334, Russia

matches the orientation of a facet and in both sides of the SF the lattice orientations are identical. In hcp crystals SFs can lie only on the c-plane—in other orientations GBs are not SFs and are high energy defects with the nearest neighbors severely disturbed while SFs in the c-plane have only the next-nearest neighbors disturbed [5].

2 Experiment

We have optically studied SFs in hcp ^{4}He crystals at 0.2 K using a sample of pure ^{4}He (only 80 ppb of ^{3}He). The shape of the crystals was investigated by using an optical setup containing a Fabry-Pérot interferometer [6]. The fused silica windows of our cylindrical copper experimental cell are horizontally aligned and we look the crystals from the top. The temperature was measured by a ^{3}He melting curve thermometer attached to the cell [7]. The same experimental setup has previously been employed for the accurate measurements of the melting pressure of ^{4}He [8, 9].

The crystals under study were nucleated by pressurizing liquid ^{4}He at a temperature of 0.2 K a few mbar above the melting pressure. The initial seed of the crystal was nucleated on the capacitor made of doubly-winded 30 μm insulated copper wire to which a voltage of about 300 V was applied. After the crystal had grown to a size of ∼1 mm, it dropped on the bottom window of the experimental cell and established its final orientation, typically with the basal c-facet oriented nearly vertical to the bottom window.

The appearance of a SF was investigated with the single hcp ^{4}He crystal shown in Fig. 1(a) which had a c-facet tilted about 7° from the vertical orientation. The orientation of the crystal was determined by calculating the normal vectors of the facets. The growth of this c-facet was seen to be very slow so that the c-facet finally extended from wall-to-wall of the experimental cell and only the height of the crystal increased. The height of the crystal finally reached almost 5 mm, which corresponds to the hydrostatic pressure difference of ∼8 Pa across the c-facet. This overpressure of 8 Pa at the bottom of the c-facet was thus the threshold overpressure that needed to be overcome in order to grow the facet which stayed at rest.

After the growth threshold had been exceeded and the crystal continued growing it was noticed that the top of the crystal had a groove parallel to the c-facet and in the place where the c-facet was just staying at rest. The groove is seen in Figs. 1(b)–1(d). We have found that the grooves created in this process are most probably due to SFs which bend the crystal surface in the same manner as GBs. Once created, the SFs were immobile and could be eliminated only by melting. The lattice orientations match in both sides of the SF, which can be seen in Figs. 1(a) and 1(b) where the direction of the contour of the c-facets matches both before and after the appearance of the SF, and in Fig. 1(d) where the orientation of the a-facets matches in both sides of the SF.

Similar grooves have been earlier observed as a result of an avalanche-like recrystallization process in which the crystal height rapidly (within less than 0.1 s) "drops" creating a SF with canyon depth of ∼0.5 mm or less [10]—equally deep canyons can be seen also in the SF pictures taken by Sasaki et al. [11]. The mechanism by which the SFs appear is discussed by Rolley et al. [12] who, trying to produce high

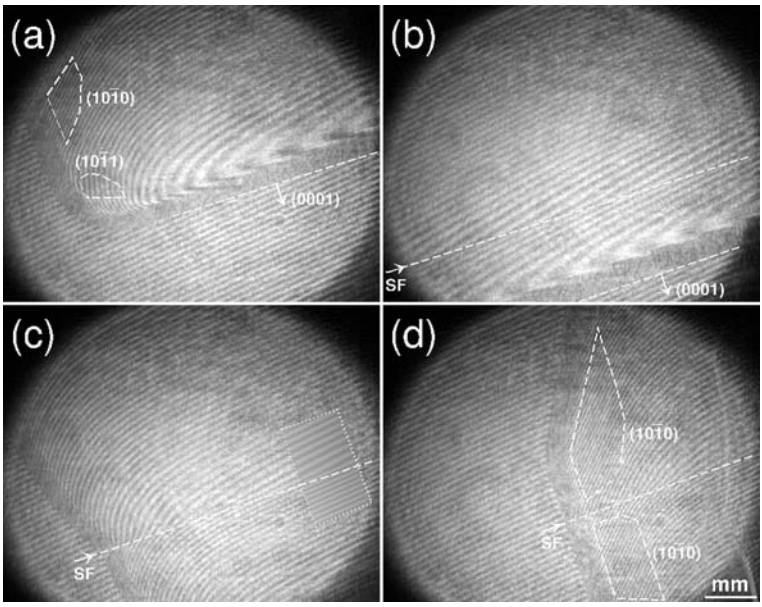

Fig. 1 ^{4}He crystal at 0.2 K (**a**) with an immobile c(0001)-facet on the steep edge of the crystal and with growing a(10$\bar{1}$0)- and s(10$\bar{1}$1)-facets—the *arrow* shows the direction of the c-axis which is 7° off from the horizon, (**b**) with a SF parallel to the growing c-facet, (**c**) with the SF on the free edge of the crystal—the *dotted region* shows a fit of the equilibrium crystal shape on both sides of the SF (see text), (**d**) with the a-facets growing at the same orientation on both sides of the SF

quality single ^{4}He crystals, found that facets may anchor to the irregularities on the wall. After exceeding the threshold, facets quickly jump into another position and a SF may be created in the process. Although we also have seen such rapid "drops" of the crystal height, we have found that the c-facet in Fig. 1 continued growing without big jumps and correspondingly the height decrease was rather slow, lasting several minutes.

The threshold overpressures of the c-facet growth in this experiment and in the burst-like growth studies by Ruutu et al. [13] are similar. This leads to the suggestion that the observed value for the growth threshold would be not only due to the absence of screw dislocations or alternatively due to large density of screw dislocations, but also due to the cell walls which have a central role in the creation of new atomic layers when spiral growth is not effective [14]. Marchenko and Parshin have found that at certain facet-to-wall contact angles it is possible to nucleate new atomic layers on c-facet even without any threshold [15]—the threshold has been observed to vanish when this contact angle decreases below ∼47° [16]. At larger contact angles there is a finite threshold, which may become small due to surface irregularities of the rough cell wall.

The appearance of the SF and the subsequent growth of the c-facet cannot be explained with the presence of screw dislocations only. Before the appearance of the SF the threshold overpressure of the c-facet growth would correspond to the average distance of 35 μm between screw dislocations, but later the decreasing crystal height

indicated diminishing growth threshold and correspondingly decreasing density of screw dislocations. It is unlikely that the densities of the screw dislocations on the two sides of the SF would not match, since screw dislocations cannot simply terminate on the SF. At the SF the screw dislocations can probably somehow reconnect, which however distorts the SF so that it is not anymore a simple SF but some more complicated structure. It is therefore possible that the c-facet had no screw dislocations and the nucleation of new atomic layers on the c-facet took place on the rough cell walls.

3 Equilibrium Crystal Shape with Anisotropic Surface Stiffness

The groove which SF produces on the crystal surface is in a quasi-equilibrium with liquid and can be described by the Laplace–Young equation [17],

$$\Delta\rho_{ls}\, g(h - h_0) = -(\gamma_1\kappa_1 + \gamma_2\kappa_2), \tag{1}$$

where h is the vertical position of the liquid-solid interface, g is the acceleration of gravity, $\Delta\rho_{ls}$ is the density difference between liquid and solid ^{4}He, and γ_i is the value of the surface stiffness component corresponding to the principal curvature κ_i.

We consider situation where one of the principal curvatures κ_i is very small and the surface stiffness $\gamma(\theta)$ is anisotropic. In this case equation (1) reduces into one dimension,

$$(h - h_0) = -\frac{\gamma(\theta)}{\Delta\rho_{ls}\, g}\,\frac{x''(h)}{[1 + x'(h)^2]^{3/2}}. \tag{2}$$

Here $x'(h) = \tan(\theta - \theta_{\text{tilt}})$ and θ is the angle subtended by the normal of the surface and the normal of the SF which is tilted by the angle θ_{tilt} with respect to vertical. The value of the surface stiffness $\gamma(\theta)$ has been taken from the measurements on the melting-freezing waves by Andreeva and Keshishev [18] in the range that covers the orientations of the fitted surface profile, namely the range $65 < \theta < 90°$ from the [0001] orientation to the [11$\bar{2}$0] orientation. The differential equation (2) was solved numerically.

The surface profiles on both sides of the SF were fitted with (2). The cross-section of the fitted surface profile is shown in Fig. 2 which illustrates the depth of the groove

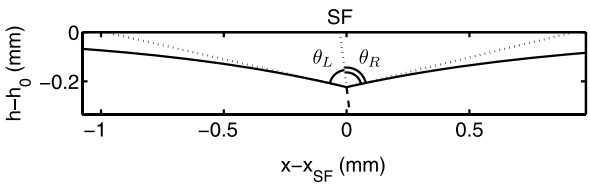

Fig. 2 The cross section of the fitted equilibrium crystal shape (*solid line*) near the SF (*dashed line*) tilted with respect to vertical by $\theta_{\text{tilt}} = 7°$. The tangential planes (*dotted lines*) of the crystal surface and of the SF are drawn for the lowest point of the groove which the SF creates. The dihedral angle $(\theta_L + \theta_R)$ of the groove is the sum of the contact angles θ_L and θ_R subtended by the normal of the crystal surface and the normal of the SF

$|h(0) - h_0|$ and the contact angles θ_L and θ_R subtended by the normal of the crystal surface and the normal of the SF. In the fitted area of interest shown in Fig. 1(c), the position $h(0)$ of the groove and the amplitude and phase of the interference pattern were also fitted at the same time—in the interference pattern there is also a linearly changing phase component which was separately found out by a fit to an interferogram containing only liquid. By this manner the profile of the crystal surface near the SF at a fixed orientation and contact angles θ_L and θ_R have been found.

4 Stacking Fault Energy

The SF energy ϵ_{SF} in the case of anisotropic surface tension [15] is

$$\epsilon_{\mathrm{SF}} = \alpha(\theta_L)\cos\theta_L + \alpha'(\theta_L)\sin\theta_L + \alpha(\theta_R)\cos\theta_R + \alpha'(\theta_R)\sin\theta_R. \tag{3}$$

The angular dependence of the surface tension $\alpha(\theta)$ and its derivative $\alpha'(\theta)$ were calculated by numerically solving the differential equation which relates the surface tension $\alpha(\theta)$ and surface stiffness $\gamma(\theta)$ [18],

$$\alpha(\theta) + \partial^2\alpha(\theta)/\partial\theta^2 = \gamma(\theta). \tag{4}$$

The necessary boundary conditions were fixed according to the known value of the energy of an elementary step on c-facet (β/a) [14],

$$\alpha'(0) = (\beta/a) = 14\ \mu\mathrm{J/m}^2,$$

and the condition of zero step energy in the $[11\bar{2}0]$ direction where no facet has been reported,

$$\alpha'(\pi/2) = 0.$$

Although we have observed some singularity in the $[11\bar{2}0]$ direction, it is weak and the step energy can be estimated to be below $\lesssim 1\ \mu\mathrm{J/m}^2$, which does not significantly change the values for $\alpha(\theta)$ and its derivative $\alpha'(\theta)$.

The values of the two contact angles for the SF shown in Fig. 1 were found to be $\theta_L = 70 \pm 3°$ and $\theta_R = 85 \pm 3°$ with several fits on different areas, the dihedral angle for the SF is thus $155 \pm 5°$. The values calculated for the surface tension are $\alpha(\theta_L) = \alpha(\theta_R) = 0.18\ \mathrm{mJ/m}^2$, and for its derivatives $\alpha'(\theta_L) = -2.8\ \mu\mathrm{J/m}^2$ and $\alpha'(\theta_R) = 1.7\ \mu\mathrm{J/m}^2$. The value given by equation (3) for the SF energy is thus $\epsilon_{\mathrm{SF}} = (0.07 \pm 0.02)\ \mathrm{mJ/m}^2$. The obtained value for the SF energy is a bit smaller than the previous rough estimate of 0.1–0.2 $\mathrm{mJ/m}^2$ based on the canyon depth of ∼0.5 mm [10]—for the analysed crystal the canyon depths were 0.20–0.25 mm. The isotropic surface tension approximation for the SF energy,

$$\epsilon_{\mathrm{SF}} = 2\langle\alpha\rangle\cos\langle\theta\rangle, \tag{5}$$

gives only 2% larger value for the SF energy, which fits within the experimental error.

Equation (2) for the crystal profile can be used only if the orientation of the crystal is known, the groove is far from facets and the approximation of a 1D surface profile

is valid. We have found however that far from facets the derivatives α' in the exact equation (3) are small and instead one can use approximation (5) for the SF energy. For different grooves on other crystals we have obtained the same dihedral angle $2\theta = 155 \pm 5^\circ$ giving the same value for the SF energy.

5 Discussion

We have measured the SF energy for a ^{4}He crystal at 0.2 K. The measured SF energy, $\epsilon_{SF} = (0.07 \pm 0.02)$ mJ/m^2, is about 0.4 of the value of the surface tension, which falls between 0.16–0.18 mJ/m^2 for different orientations [14]. Compared to GBs, the SF energy is found to be about 0.2 of the recently reported energy of GBs [11].

In the growth process where the SF was created, the growth threshold of the c-facet was ∼8 Pa which is similar to the overpressures observed in the burst-like creation of new atomic layers [13]. The role of cell walls in creation of new atomic layers and similar threshold overpressures suggest that the burst-like growth might be accompanied by the creation of SFs. Nevertheless, the mechanism of the burst-like creation of new atomic layers remains unexplained.

Acknowledgements This work was supported by the EC-funded ULTI project, Transnational Access Programme FP6 (contract #RITA-CT-2003-505313), and by the Academy of Finland (Finnish Centre of Excellence Programme 2006–2011, and Visitors Programmes 121895 and 127710).

References

1. S. Balibar, F. Caupin, Condens. Matter **20**, 173201 (2008)
2. E. Kim, M. Chan, Nature **427**, 225 (2004)
3. E. Kim, M. Chan, Science **305**, 1941 (2004)
4. S. Balibar, Physics **1**, 18 (2008)
5. W.T. Read, *Dislocations in Crystals* (McGraw-Hill, New York, 1953)
6. V. Tsepelin, H. Alles, J.P.H. Härme, R. Jochemsen, A.Ya. Parshin, G. Tvalashvili, J. Low Temp. Phys. **121**, 695 (2000)
7. R.L. Rusby, M. Durieux, A.L. Reesink, R.P. Hudson, G. Schuster, M. Kühne, W.E. Fogle, R.J. Soulen, E.D. Adams, J. Low Temp. Phys. **112**, 633 (2002)
8. I.A. Todoshchenko, H. Alles, J. Bueno, H.J. Junes, A.Ya. Parshin, V. Tsepelin, Phys. Rev. Lett. **97**, 165302 (2006)
9. I.A. Todoshchenko, H. Alles, H.J. Junes, A.Ya. Parshin, V. Tsepelin, Pis'ma ZhETF **85**, 555 (2007) [JETP Lett. **85**, 454 (2007)]
10. A.Ya. Parshin, *Low Temperature Physics* (MIR, Moscow, 1985)
11. S. Sasaki, F. Caupin, S. Balibar, Phys. Rev. Lett. **99**, 205302 (2007)
12. E. Rolley, C. Guthmann, E. Chevalier, S. Balibar, J. Low Temp. Phys. **99**, 851 (1995)
13. J.P. Ruutu, P.J. Hakonen, A.V. Babkin, A.Ya. Parshin, G. Tvalashvili, J. Low Temp. Phys. **112**, 117 (1998)
14. S. Balibar, H. Alles, A.Ya. Parshin, Rev. Mod. Phys. **77**, 317 (2005)
15. V.I. Marchenko, A.Ya. Parshin, Pis'ma ZhETF **83**, 485 (2006) [JETP Lett. **83**, 416 (2006)]
16. K.O. Keshishev, V.N. Sorokin, D.B. Shemyatikhin, Pis'ma ZhETF **85**, 213 (2007) [JETP Lett. **85**, 179 (2007)]
17. P. Nozières, *Solids Far from Equilibrium* (Cambridge University Press, Cambridge, 1991)
18. O.A. Andreeva, K.O. Keshishev, Phys. Scr. T **39**, 352 (1991)